62
Research paper
Doi 10.61892/STP202601019K
ISSN 2566-4484

Nevenka Kolarevic, University of Belgrade - Faculty of Civil Engineering, nevenka@grf.bg.ac.rs
Marija Nefovska-Danilović, University of Belgrade - Faculty of Civil Engineering, marija@grf.bg.ac.rs

FREE VIBRATION STUDY OF CIRCULAR CYLINDRICAL SHELLS USING DYNAMIC STIFFNESS METHOD

Abstract:

This paper provides an overview of the authors' research on the free vibration analysis of circular cylindrical shells using the Dynamic stiffness method. Exact frequency-dependent dynamic stiffness matrices, derived from Flügge shell theory and its shear-deformable extension, enable highly accurate prediction of modal properties without the need for discretization. The review summarizes the main theoretical contributions from the authors' previous work and presents parametric studies, offering a unified perspective on DSM applications to shell-like structures and outlining directions for future research.

Keywords: Dynamic Stiffness Method; Free Vibration; Cylindrical Shells; Flügge Theory; Shear Deformation

АНАЛИЗА СЛОБОДНИХ ВИБРАЦИЈА КРУЖНИХ ЦИЛИНДРИЧНИХ ЉУСКИ ПРИМЕНОМ МЕТОДЕ ДИНАМИЧКЕ КРУТОСТИ

Сажетак:

Овај рад даје преглед истраживања ауторки у области анализе слободних вибрација кружно-цилиндричних љуски применом Методе динамичке крутости. Тачне, фреквентно зависне матрице динамичке крутости, које су изведене су на основу Flügge теорије љуски и њене проширене формулације која укључује утицаје смичуће деформације и ротационе инерције, омогућавају веома прецизно одређивање модалних карактеристика без потребе за физичком дискретизацијом. Рад сумира главне теоријске доприносе из ранијих радова ауторки у овој области и кроз нумеричке примере илуструје примену Методе динамичке крутости на конструкције типа љуски и указује на правце будућих истраживања

Кључне ријечи: Метод динамичке крутости, Слободне вибрације, цилиндричне љуске, Flügge теорија

1. INTRODUCTION

Circular cylindrical shells play an important role in structural design. They can be found in various engineering applications such as water tanks, tunnels, ventilation ducts, pipelines, silos, and parts of fuselages in aerospace structures. Additionally, they are widely used in marine and offshore structures (e.g., submarine hulls, ship structures), as well as in civil engineering, including cooling towers and storage reservoirs. Due to their high strength-to-weight ratio and ability to withstand complex loading conditions, cylindrical shells represent an efficient and reliable structural solution in many industries.

As lightweight structures, cylindrical shells are highly sensitive to dynamic loading conditions, which can lead to excessive vibrations or even structural failure. Therefore, reliable determination of modal properties is essential in their design and analysis.

The Dynamic stiffness method (DSM) stands out as a powerful approach that combines the advantages of both analytical formulations and the Finite element method (FEM). The frequency-dependent dynamic stiffness (DS) matrices are derived from strong-form solutions of the governing differential equations (GDEs) of motion, unlike in FEM where discretization and the use of polynomial interpolation functions introduce approximation errors. At the same time, DSM retains the assembly procedure inherent to FEM, which enables efficient modeling of complex systems, as well as straightforward implementation of various boundary conditions—capabilities that are typically limited in purely analytical solutions.

Langley [1] was among the first to apply the DSM to shell vibrations, analyzing a singly curved, orthogonally stiffened shell with constant curvature and simply supported edges. Leung [2], [3] extended DSM applications to toroidal shells using the Donnell–Mushtari–Vlasov theory, as well as to uniform and non-uniform circular cylindrical shells governed by the Donnell–Mushtari and Flügge equations. Casimir et al. [4] developed the DS matrix for axisymmetric thick shells including rotary inertia and shear effects, which was further extended by Thinh and Nguyen [5] to laminated composite cylindrical shells. Tounsi [6] formulated the DS matrix for axisymmetric shells stiffened with multiple circumferential stiffeners, while Fazzolari [7] derived it for doubly curved laminated composite shallow shells with two opposite edges simply supported, combining exact free vibration solutions and higher-order shear deformation theory. The authors' contributions [8], [9], [10] present a unified approach for deriving DS matrices based on Flügge shell theory for closed and open circular cylindrical shells, and its shear-deformable extension for closed shells, applicable to arbitrary boundary conditions. This methodology can also be applied to a wide range of shell-like structures, including shells with stepped thickness, shells with intermediate supports, and barrel roofs.

In this paper, the fundamental principles of the DSM are presented, followed by a detailed review of the frequency-dependent DS matrices for cylindrical shells developed by the authors in their previous research. Selected numerical examples are provided to demonstrate the accuracy and efficiency of the proposed formulations in free vibration analysis.

2. DYNAMIC STIFFNESS FORMULATION

DSM is based on the exact solution of the GDEs derived for the corresponding elastodynamic problem in the frequency domain. The key element of this method is the DS matrix, which relates the generalized forces and displacements at the element boundaries. Two types of cylindrical shell geometries are considered: closed and open circular cylindrical shells (Fig. 1). The GDEs for the free vibration problem are formulated using Flügge shell theory and its shear-deformable extension.

The solution of the GDEs depends on the element geometry. For a closed circular cylindrical shell, a closed-form solution is obtained, whereas for an open circular cylindrical shell, a superposition and projection method must be used. Although the solution is analytical, it is expressed in the form of a Fourier series, and thus depends on the number of terms used. Consequently, a convergence study must be performed.

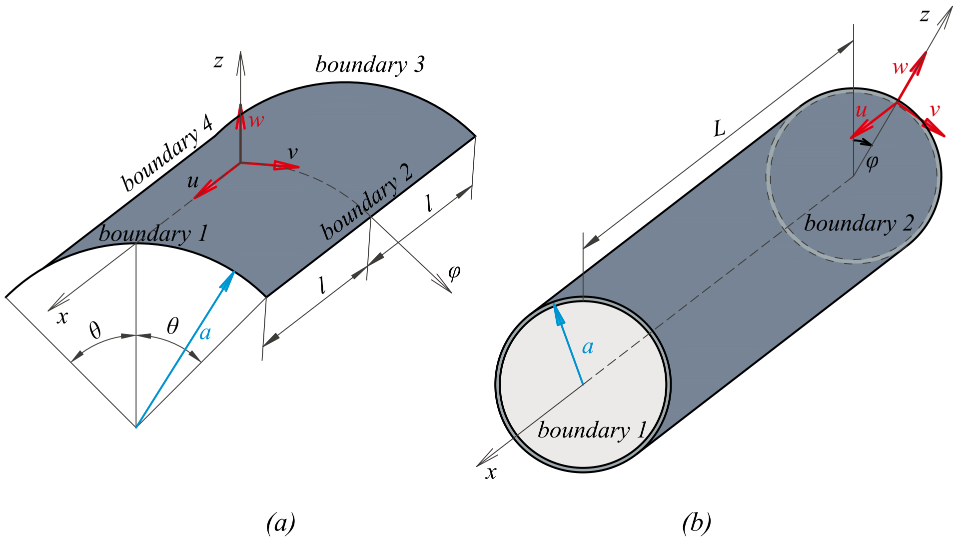

Figure 1. Geometry and coordinate system for an (a) open circular cylindrical shell and (b) circular cylindrical shell (drawing by author, created in AutoCAD)

2.1. FLÜGGE SHELL THEORY AND ITS SHEAR-DEFORMABLE EXTENSION

The displacement field of an arbitrary point (*x, y, z*) at an arbitrary time *t* is given as:

$$\begin{aligned} u(x,\varphi,z,t) &= u^0(x,\varphi,t) + z\psi_x(x,\varphi,t) \\ v(x,\varphi,z,t) &= v^0(x,\varphi,t) + z\psi_\varphi(x,\varphi,t) \\ w(x,\varphi,z,t) &= w^0(x,\varphi,t) \end{aligned} \tag{1}$$

Where $u^0(x,\varphi,t)$, $v^0(x,\varphi,t)$ and $w^0(x,\varphi,t)$ denote the mid-surface displacement components in the axial, tangential, and radial direction, respectively. The quantities ψ_x and ψ_φ represent the rotations of the normal to the mid-surface about the φ and x axis, respectively.

In classical thin-shell theory (Flügge theory), these rotations are not independent variables. Instead, they are expressed in terms of the displacement components u, v, and w. For a circular cylindrical shell, the rotations are given by:

$$\begin{aligned} \psi_x(x,\varphi) &= -\frac{\partial w^0}{\partial x} \\ \psi_\varphi(x,\varphi) &= \frac{1}{a}\left(v^0 - \frac{\partial w^0}{\partial \varphi}\right) \end{aligned} \tag{2}$$

where a is the radius of the shell.

In contrast, in shear-deformable shell theories, the rotations ψ_x and ψ_φ become additional independent variables, allowing transverse shear deformation to be included in the formulation.

The equations of motion based on Flügge shell theory can be written as [11]:

$$
\begin{aligned}
&\frac{\partial N_x}{\partial x}+\frac{1}{a}\frac{\partial N_{\varphi x}}{\partial \varphi}+q_x=0 && (a)\\
&\frac{1}{a}\frac{\partial N_\varphi}{\partial \varphi}+\frac{\partial N_{x\varphi}}{\partial x}+\frac{Q_\varphi}{a}+q_\varphi=0 && (b)\\
&-\frac{N_\varphi}{a}+\frac{\partial Q_x}{\partial x}+\frac{1}{a}\frac{\partial Q_\varphi}{\partial \varphi}+q_z=0 && (c)\\
&\frac{\partial M_x}{\partial x}+\frac{1}{a}\frac{\partial M_{\varphi x}}{\partial \varphi}-Q_x+m_\varphi=0 && (d)\\
&\frac{1}{a}\frac{\partial M_\varphi}{\partial \varphi}+\frac{\partial M_{x\varphi}}{\partial x}-Q_\varphi+m_x=0 && (f)
\end{aligned}
\tag{3}
$$

In Eqs. (3), q_x , q_φ and q_z are the components of the inertial force resultant in the axial, tangential and radial direction, respectively, while m_φ and m_x are the components of the inertial moment resultant in the tangential and axial direction, respectively. These quantities are given by the following equations for thin and for moderately thick shell theory:

$$
\begin{array}{ll}
\underline{\textbf{Thin shell theory}} & \underline{\textbf{Moderately thick shell theory}}\\
q_x=-\rho h\dfrac{\partial^2 u^0}{\partial t^2} & q_x=-\rho h\dfrac{\partial^2 u^0}{\partial t^2}-\dfrac{\rho h^3}{12a}\dfrac{\partial^2 \psi_x}{\partial t^2}\\
q_\varphi=-\rho h\dfrac{\partial^2 v^0}{\partial t^2} & q_\varphi=-\rho h\dfrac{\partial^2 v^0}{\partial t^2}-\dfrac{\rho h^3}{12a}\dfrac{\partial^2 \psi_\varphi}{\partial t^2}\\
q_z=-\rho h\dfrac{\partial^2 w^0}{\partial t^2} & q_z=-\rho h\dfrac{\partial^2 w^0}{\partial t^2}\\
m_x=0 & m_x=-\dfrac{\rho h^3}{12a}\dfrac{\partial^2 v^0}{\partial t^2}-\dfrac{\rho h^3}{12}\dfrac{\partial^2 \psi_\varphi}{\partial t^2}\\
m_\varphi=0 & m_\varphi=-\dfrac{\rho h^3}{12a}\dfrac{\partial^2 u^0}{\partial t^2}-\dfrac{\rho h^3}{12}\dfrac{\partial^2 \psi_x}{\partial t^2}
\end{array}
\tag{4}
$$

where ρ is the mass density and h is the shell thickness.

By applying the strain-displacement relations and the expressions for force and moment resultants from Flügge’s shell theory, as presented in [11], the following force-displacement relationship are obtained:

Thin shell theory:

$$
\begin{aligned}
&N_x = D\left[\frac{\partial u^0}{\partial x} + \frac{\nu}{a}\left(w^0 + \frac{\partial v^0}{\partial \varphi}\right) - ka\frac{\partial^2 w^0}{\partial x^2}\right]\\
&N_\varphi = D\left[\frac{1}{a}\left(w^0 + \frac{\partial v^0}{\partial \varphi}\right) + \nu\frac{\partial u^0}{\partial x}\right] + \frac{K}{a^3}\left(\frac{\partial^2 w^0}{\partial \varphi^2} + w^0\right)\\
&N_{x\varphi} = \frac{D(1-\nu)}{2}\left(\frac{1}{a}\frac{\partial u^0}{\partial \varphi} + \frac{\partial v^0}{\partial x}\right) + \frac{K(1-\nu)}{2a^2}\left(\frac{\partial v^0}{\partial x} - \frac{\partial^2 w^0}{\partial x \partial \varphi}\right)\\
&N_{\varphi x} = \frac{D(1-\nu)}{2}\left(\frac{1}{a}\frac{\partial u^0}{\partial \varphi} + \frac{\partial v^0}{\partial x}\right) + \frac{K(1-\nu)}{2a^2}\left(\frac{1}{a}\frac{\partial u^0}{\partial \varphi} + \frac{\partial^2 w^0}{\partial x \partial \varphi}\right)\\
&M_x = -K\left[\frac{\partial^2 w^0}{\partial x^2} + \frac{\nu}{a^2}\left(\frac{\partial^2 w^0}{\partial \varphi^2} - \frac{\partial v^0}{\partial \varphi}\right) - \frac{1}{a}\frac{\partial u^0}{\partial x}\right];\; M_{x\varphi} = -\frac{K(1-\nu)}{a}\left(\frac{\partial^2 w^0}{\partial x \partial \varphi} - \frac{\partial v^0}{\partial x}\right)\\
&M_\varphi = -K\left[\frac{1}{a^2}\left(\frac{\partial^2 w^0}{\partial \varphi^2} + w^0\right) + \nu\frac{\partial^2 w^0}{\partial x^2}\right];\; M_{\varphi x} = -\frac{K(1-\nu)}{2a}\left(2\frac{\partial^2 w^0}{\partial x \partial \varphi} - \frac{\partial v^0}{\partial x} + \frac{1}{a}\frac{\partial u^0}{\partial \varphi}\right)
\end{aligned}
\tag{5}
$$

Moderately thick shell theory:

$$
\begin{aligned}
&N_x = D\left[\frac{\partial u^0}{\partial x} + \frac{\nu}{a}\left(w^0 + \frac{\partial v^0}{\partial \varphi}\right) + ka\frac{\partial \psi_x}{\partial x}\right] && N_\varphi = D\left[\left(\frac{w^0}{a} + \frac{\partial v^0}{a\partial \varphi}\right)(1+k) + \nu\frac{\partial u^0}{\partial x} - k\frac{\partial \psi_\varphi}{\partial \varphi}\right]\\
&N_{x\varphi} = \frac{D(1-\nu)}{2}\left(\frac{\partial u^0}{a\partial \varphi} + \frac{\partial v^0}{\partial x} + ka\frac{\partial \psi_\varphi}{\partial x}\right) && N_{\varphi x} = \frac{D(1-\nu)}{2}\left[\frac{\partial u^0}{a\partial \varphi} + \frac{\partial v^0}{\partial x} + k\left(\frac{\partial u^0}{a\partial \varphi} - \frac{\partial \psi_x}{\partial \varphi}\right)\right]\\
&Q_x = Dk_1\left(\frac{\partial w^0}{\partial x} + \psi_x\right) && Q_\varphi = Dk_1(1+k)\left(\frac{\partial w^0}{a\partial \varphi} - \frac{v^0}{a} + \psi_\varphi\right)\\
&M_x = K\left(\frac{\partial \psi_x}{\partial x} + \nu\frac{\partial \psi_\varphi}{a\partial \varphi} + \frac{\partial u^0}{a\partial x}\right) && M_\varphi = K\left[\frac{\partial \psi_\varphi}{a\partial \varphi} + \nu\frac{\partial \psi_x}{\partial x} - \frac{1}{a^2}\left(\frac{\partial v^0}{\partial \varphi} + w^0\right)\right]\\
&M_{x\varphi} = \frac{K(1-\nu)}{2}\left(\frac{\partial \psi_x}{a\partial \varphi} + \frac{\partial \psi_\varphi}{\partial x} + \frac{\partial v^0}{a\partial x}\right) && M_{\varphi x} = \frac{K(1-\nu)}{2}\left(\frac{\partial \psi_x}{a\partial \varphi} + \frac{\partial \psi_\varphi}{\partial x} - \frac{\partial u^0}{a^2\partial x}\right)
\end{aligned}
\tag{6}
$$

where: $k = \dfrac{h^2}{12a^2}$, ν is the Poisson's ratio, $k_1 = \nu_1\kappa^2$, κ^2 is the shear correction factor and $\nu_1 = (1-\nu)/2$, E is the Young's modulus of elasticity, $K = Eh^3/12(1-\nu^2)$ is the flexural stiffness and $D = Eh/(1-\nu^2)$ is the membrane stiffness of the cylindrical shell.

By substituting Eqs. (6) into Eqs. (3), the GDEs of motion based on Flügge shell theory, accounting for the effects of shear deformation and rotary inertia can be expressed as:

$$\left[\mathrm{L}^{MT}\right]\left\{u_i^{MT}\right\} = \{0\} \tag{7}$$

where $\left[\mathbf{L}^{MT}\right]$ is the fifth-order matrix differential operator for the moderately thick shell theory, whose components $\mathbf{L}_{ij}$ are given in [9], and $\left\{u_i^{MT}\right\}$ represents the generalized displacement vector of this formulation:

$$\left\{u_i^{MT}\right\}^T = \left\{u^0(x,\varphi,t) \quad v^0(x,\varphi,t) \quad w^0(x,\varphi,t) \quad \psi_x(x,\varphi,t) \quad \psi_\varphi(x,\varphi,t)\right\} \tag{8}$$

In the thin shell theory, the shear forces Q_x and Q_φ cannot be expressed directly in the term of displacement as a consequence of neglecting shear deformation. Instead, they are expressed in terms of bending moments using Eqs. (3.d) and (3.f):

$$Q_x = \frac{\partial M_x}{\partial x} + \frac{1}{a}\frac{\partial M_{\varphi x}}{\partial \varphi} \qquad Q_\varphi = \frac{1}{a}\frac{\partial M_\varphi}{\partial \varphi} + \frac{\partial M_{x\varphi}}{\partial x} \tag{9}$$

The expressions for the shear forces from Eq. (9) are substituted into Eqs. (3.a) to (3.c). After further substitution of the force and moment resultants in terms of u^0, v^0 and w^0 from Eqs. (5), the following governing differential equations are obtained:

$$\left[\mathrm{L}^{Thin}\right]\left\{u_i^{Thin}\right\} = \{0\} \tag{10}$$

where $\left[\mathrm{L}^{Thin}\right]$ is the third-order matrix differential operator for the thin shell theory, whose components L_{ij} are given in [10], and $\left\{u_i^{Thin}\right\}$ is the associated generalized displacement vector:

$$\left\{u_i^{Thin}\right\}^T = \left\{u^0(x,\varphi,t) \quad v^0(x,\varphi,t) \quad w^0(x,\varphi,t)\right\} \tag{11}$$

2.2. GENERAL SOLUTION

By applying the method of separation of variables, the general solution to systems (7) and (10) can be written in the following form:

$$\begin{aligned} &u^0(x,\varphi,t) = \hat{u}(x,\varphi)e^{i\omega t}; \ v^0(x,\varphi,t) = \hat{v}(x,\varphi)e^{i\omega t}; \ w^0(x,\varphi,t) = \hat{w}(x,\varphi)e^{i\omega t} \\ &\psi_x(x,\varphi,t) = \hat{\psi}_x(x,\varphi)e^{i\omega t}; \ \psi_\varphi(x,\varphi,t) = \hat{\psi}_\varphi(x,\varphi)e^{i\omega t} \end{aligned} \tag{12}$$

In this way, the time variable is eliminated from the differential equations. Consequently, the components of the displacement vector in time domain become functions of the spatial coordinates x and φ only. The solution for the unknown functions now depends on the geometry of the shell. For a closed circular cylindrical shell, the amplitudes of the displacement components in the frequency domain $\hat{u}$, $\hat{v}$, $\hat{w}$, $\hat{\psi}_x$ and $\hat{\psi}_\varphi$ must satisfy the periodicity condition in the circumferential direction. Therefore, the solution is expressed in the form of an infinite Fourier series:

Thin shell theory:

$$\begin{aligned} \hat{u}(x,\varphi) &= \sum_{m=0}^{\infty} U_m^1(x)\cos(m\varphi) + \sum_{m=1}^{\infty} U_m^2(x)\sin(m\varphi) \\ \hat{v}(x,\varphi) &= \sum_{m=1}^{\infty} V_m^1(x)\sin(m\varphi) + \sum_{m=0}^{\infty} V_m^2(x)\cos(m\varphi) \\ \hat{w}(x,\varphi) &= \sum_{m=0}^{\infty} W_m^1(x)\cos(m\varphi) + \sum_{m=1}^{\infty} W_m^2(x)\sin(m\varphi) \end{aligned} \tag{13}$$

Moderately thick shell theory:

$$\begin{aligned} \hat{u}(x,\varphi) &= \sum_{m=0}^{\infty} U_m^1(x)\cos(m\varphi) + \sum_{m=1}^{\infty} U_m^2(x)\sin(m\varphi) \\ \hat{v}(x,\varphi) &= \sum_{m=1}^{\infty} V_m^1(x)\sin(m\varphi) + \sum_{m=0}^{\infty} V_m^2(x)\cos(m\varphi) \\ \hat{w}(x,\varphi) &= \sum_{m=0}^{\infty} W_m^1(x)\cos(m\varphi) + \sum_{m=1}^{\infty} W_m^2(x)\sin(m\varphi) \\ \hat{\psi}_x(x,\varphi) &= \sum_{m=0}^{\infty} \Psi_{xm}^1(x)\cos(m\varphi) + \sum_{m=1}^{\infty} \Psi_{xm}^2(x)\sin(m\varphi) \\ \hat{\psi}_\varphi(x,\varphi) &= \sum_{m=1}^{\infty} \Psi_{\varphi m}^1(x)\sin(m\varphi) + \sum_{m=0}^{\infty} \Psi_{\varphi m}^2(x)\cos(m\varphi) \end{aligned} \tag{14}$$

where m is the circumferential wave number. When the boundary conditions are axisymmetric, the solutions for different harmonics become uncoupled. Thus, the solutions for each harmonic m can

be obtained independently. In this manner, the exact analytical solution corresponding to the adopted elastodynamic theory is obtained. A detailed derivation is provided in [8] and [9].
In contrast, for an open circular cylindrical shell, the periodicity condition in the circumferential direction in no longer valid. Therefore, the solution becomes more complex, and the superposition method is applied. The superposition method decomposes an arbitrary deformation into four symmetry contributions. For the thin shell theory, the displacement components $\hat{u}(x,\varphi)$, $\hat{v}(x,\varphi)$ and $\hat{w}(x,\varphi)$ are decomposed into four symmetry contributions: symmetric-symmetric (*SS*), symmetric - anti-symmetric (*SA*), anti-symmetric - symmetric (*AS*) and anti-symmetric - anti-symmetric (*AA*):

$$\begin{aligned}\hat{u}(x,\varphi) &= \hat{u}^{SS}(x,\varphi)+\hat{u}^{SA}(x,\varphi)+\hat{u}^{AS}(x,\varphi)+\hat{u}^{AA}(x,\varphi)\\ \hat{v}(x,\varphi) &= \hat{v}^{SS}(x,\varphi)+\hat{v}^{SA}(x,\varphi)+\hat{v}^{AS}(x,\varphi)+\hat{v}^{AA}(x,\varphi)\\ \hat{w}(x,\varphi) &= \hat{w}^{SS}(x,\varphi)+\hat{w}^{SA}(x,\varphi)+\hat{w}^{AS}(x,\varphi)+\hat{w}^{AA}(x,\varphi)\end{aligned} \tag{15}$$

The solution is obtained separately for each symmetry contribution.

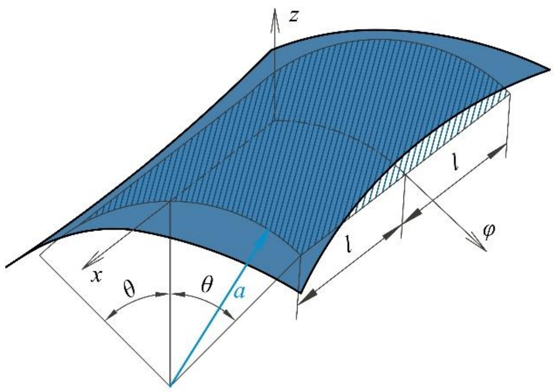

Figure 2. Symmetric–symmetric deformation of an open circular cylindrical shell (drawing by author, created in AutoCAD)

For the *SS* deformation of the shell element shown in Fig. 2, the solution is assumed in the form of Fourier series truncated to *M* terms:

$$\begin{aligned}\hat{u}^{SS}(x,\varphi) &= \sum_{m=0}^{M} {}^{1}U_m^{SS}(x)\cos(\alpha_m\varphi) + \sum_{m=1}^{M} {}^{2}U_m^{SS}(\varphi)\sin(\beta_m x)\\ \hat{v}^{SS}(x,\varphi) &= \sum_{m=1}^{M} {}^{1}V_m^{SS}(x)\sin(\alpha_m\varphi) + \sum_{m=0}^{M} {}^{2}V_m^{SS}(\varphi)\cos(\beta_m x)\\ \hat{w}^{SS}(x,\varphi) &= \sum_{m=0}^{M} {}^{1}W_m^{SS}(x)\cos(\alpha_m\varphi) + \sum_{m=0}^{M} {}^{2}W_m^{SS}(\varphi)\cos(\beta_m x)\end{aligned} \tag{16}$$

where $\alpha_m = m\pi/\theta$ and $\beta_m = m\pi/l$ are the circumferential and axial wave numbers, respectively. In this case, the solution depends on the number of terms included. In contrast to the solution for a closed circular cylindrical shell, an exact analytical solution does not exist, and the accuracy of results depends on the number of terms used. Therefore, a convergence study must be performed. A detailed derivation is provided in [10].

3. DERIVATION OF THE DYNAMIC STIFFNESS MATRIX

The DS matrix establishes the relationship between the displacement and force vectors, $\hat{\mathbf{q}}$ and $\hat{\mathbf{Q}}$, at the shell boundaries $x=0$ and $x=L$ for a closed circular cylindrical shell, and at the boundaries $x=l$ and $\varphi=\theta$ for an open circular cylindrical shell. For a closed circular cylindrical shell, the components of these vectors are shown in Figs. 3 and 4 for the thin and moderately thick shell theories, respectively, while Fig. 5 presents the corresponding quantities for an open circular cylindrical shell for the *SS* contribution.

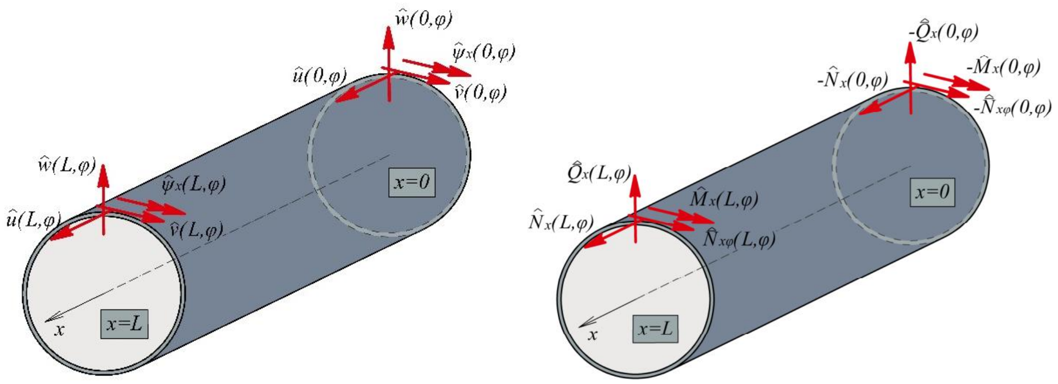

(a) (b)

Figure 3. Displacement (a) and force (b) components for thin shell theory (drawing by author, created in AutoCAD)

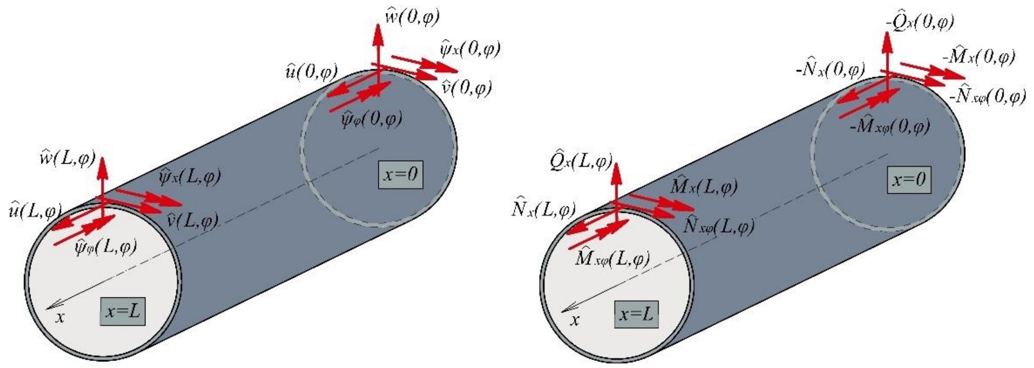

(a) (b)

Figure 4. Displacement (a) and force (b) components for moderately thick shell theory (drawing by author, created in AutoCAD)

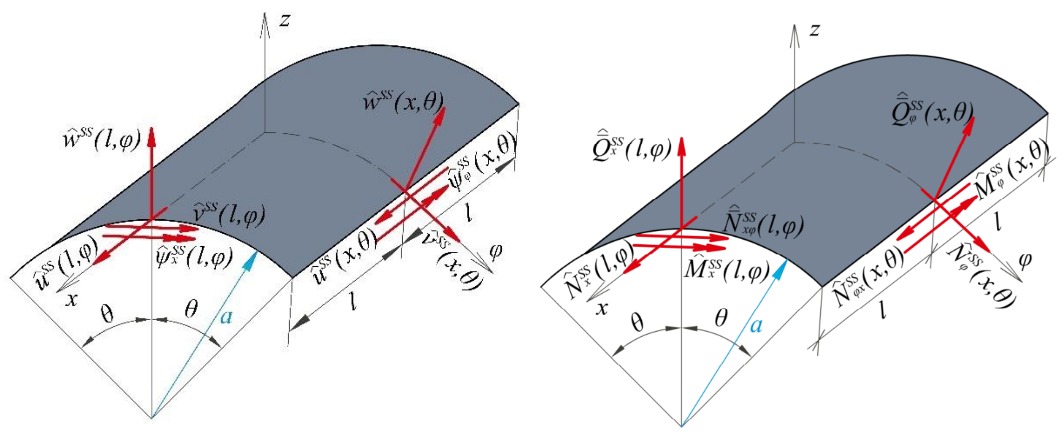

(a) (b)

Figure 5. Displacement (a) and force (b) components along the boundaries for SS contribution (thin shell theory) (drawing by author, created in AutoCAD)

A detailed derivation of DS matrix for a circular cylindrical shell, which relates the displacement and force vectors, is provided in [8] and [9]. For each circumferential harmonic *m*, the DS matrix $\mathbf{K}_{Dm}$ has dimension 8 in thin shell theory and 10 in moderately thick shell theory.

Unlike the closed shell, the boundary quantities $\hat{\mathbf{q}}^{SS}$ and $\hat{\mathbf{Q}}^{SS}$ for the open shell cannot be related in closed form, as they depend on the spatial coordinates *x* (on the boundary $\varphi = \theta$) and φ (on the boundary $x = l$). This difficulty is overcome using the projection method [12], in which all boundary quantities are expanded in a truncated set of trigonometric basis functions. Further details are provided in [10]. The resulting DS matrix for the SS contribution $\tilde{\mathbf{K}}_D^{SS}$ has dimension $8M+6$, where

M is the number of retained terms. DS matrices for the remaining symmetry contributions, $\tilde{\mathbf{K}}_D^{SA}$, $\tilde{\mathbf{K}}_D^{AS}$, $\tilde{\mathbf{K}}_D^{AA}$, can be derived in an analogous manner.

Finally, the DS matrix of a completely free open circular cylindrical shell $\tilde{\mathbf{K}}_D$ is assembled from the previously obtained *SS*, *SA*, *AS* and *AA* matrices, following the procedure described in [10]. The resulting matrix $\tilde{\mathbf{K}}_D$ has dimension $32M+12$.

4. . BOUNDARY CONDITIONS, NATURAL FREQUENCIES AND MODE SHAPES

When the DS matrix is determined, a global DS matrix of the structure can be obtained. The procedure is similar to that of FEM, except that continuous elements are connected at the boundaries, instead at nodes. Some examples of shell-like structures that can be analyzed using formulated DS elements are given in Fig 6 and 7.

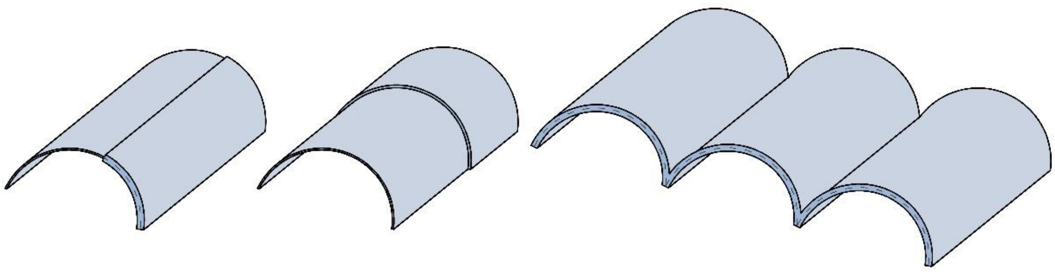

Figure 6. *Open circular cylindrical shells with stepwise thickness variation and a barrel roof (drawing by author, created in AutoCAD)*

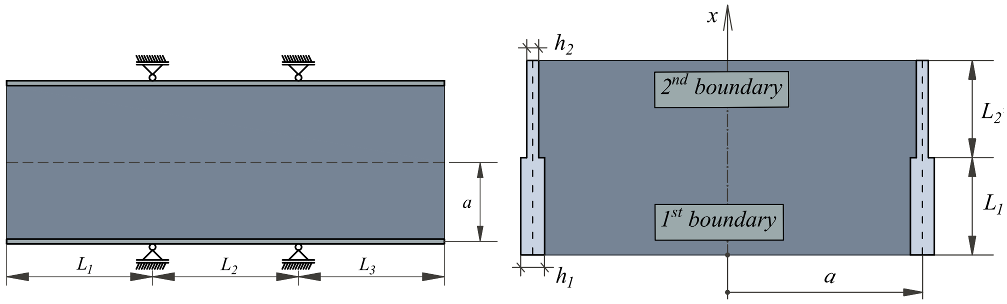

Figure 7. *Cylindrical shells with (a) intermediate ring supports and (b) stepwise thickness variation (drawing by author, created in AutoCAD)*

Once the global DS matrix is assembled, the boundary conditions are applied by removing the rows and columns corresponding to constrained displacements and rotations. In the numerical examples, only results for the most commonly used boundary conditions are presented: free, shear diaphragm, simply supported, and clamped.

Natural frequencies and mode shapes are obtained using the well-known procedure described in [10]. The natural frequencies correspond to the condition $\det(\mathbf{K}_{Dm})=0$. Since the zeros of the determinant cannot be determined analytically, a custom MATLAB code is employed to plot $1/\log\det(\mathbf{K}_{Dm})$ as a function of frequency. A typical MATLAB plot is shown in Fig. 8. An appropriate choice of the frequency step size is essential to ensure that no natural frequencies are missed.

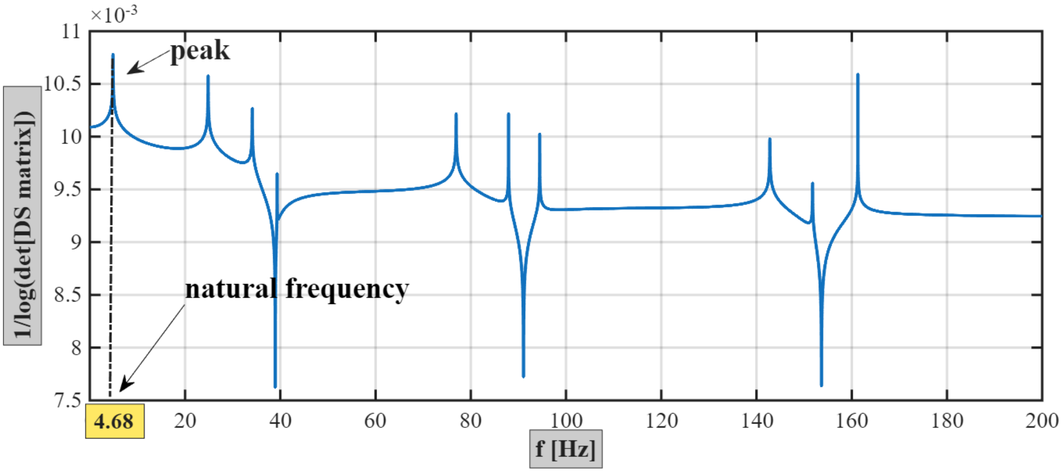

Figure 8. *Identification of natural frequencies from the dynamic stiffness matrix*

5. NUMERICAL STUDY

Example 1.
In this numerical example, the methodology presented herein has been used in the free vibration analysis of a barrel roof shown in Figure 9.

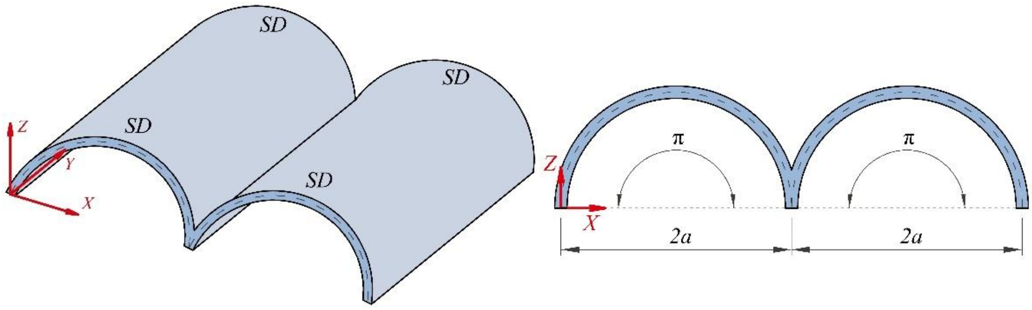

Figure 9. Disposition of a barrel roof (drawing by author, created in AutoCAD)

Two-span barrel roof, with the following geometrical characteristics of each segment: h/a =0.005, $L/a = 5$ and $2\theta = 180^o$, is modeled with two DS elements. Two opposite curved edges are chosen to be *shear diaphragm* SD ($v = w = 0$), while the edges for $X = 0$, $2a$ and $4a$ are subjected to *free* F or *simply supported* S ($u = v = w = 0$) boundary condition. Before the standard assembly procedure is carried out, the DS matrix $\mathbf{K}_{Dm}$ should be transformed from the local to the global coordinate system. Displacement transformation from the local to global coordinate system, referring to Figure 10, is given by:

$$\begin{bmatrix} U_1 \\ V_1 \\ W_1 \\ \Psi_{y,1} \\ U_2 \\ V_2 \\ W_2 \\ \Psi_{y,2} \end{bmatrix}_{8x1} = \begin{bmatrix} \cos(\theta) & 0 & -\sin(\theta) & 0 & 0 & 0 & 0 & 0 \\ 0 & 1 & 0 & 0 & 0 & 0 & 0 & 0 \\ \sin(\theta) & 0 & \cos(\theta) & 0 & 0 & 0 & 0 & 0 \\ 0 & 0 & 0 & 1 & 0 & 0 & 0 & 0 \\ 0 & 0 & 0 & 0 & \cos(\theta) & 0 & \sin(\theta) & 0 \\ 0 & 0 & 0 & 0 & 0 & 1 & 0 & 0 \\ 0 & 0 & 0 & 0 & -\sin(\theta) & 0 & \cos(\theta) & 0 \\ 0 & 0 & 0 & 0 & 0 & 0 & 0 & 1 \end{bmatrix}_{8x8} \cdot \begin{bmatrix} v_1 \\ u_1 \\ w_1 \\ \psi_{\varphi,1} \\ v_2 \\ u_2 \\ w_2 \\ \psi_{\varphi,2} \end{bmatrix}_{8x1} \tag{17}$$

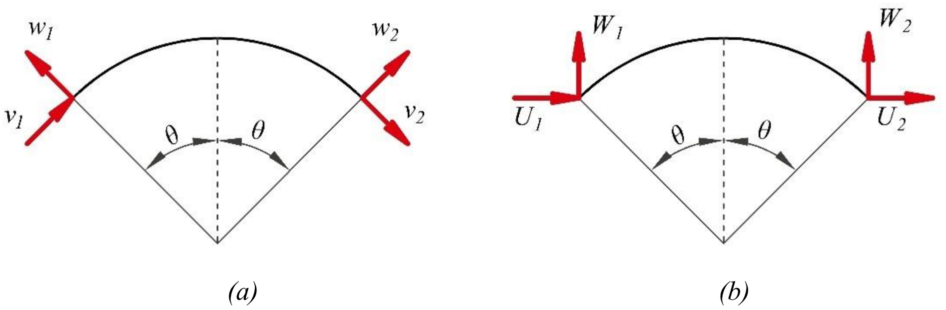

Figure 10. Displacement transformation from local (a) to global (b) coordinate system (drawing by author, created in AutoCAD)

When the transformation matrix is defined, the DS matrix in the global coordinate system can be computed from the following expression:

$$\mathbf{K}_{Dm}^{G} = \mathbf{T}^{*} \cdot \mathbf{K}_{Dm} \cdot \left(\mathbf{T}^{*}\right)^{T} \tag{18}$$

Table 1 gives the first five dimensionless natural frequencies $\Omega = \omega a^2 \sqrt{\rho\left(1-\nu^2\right)/E}$ computed by the presented method as well as the results from Abaqus, where 50400 S4R finite elements are used for modeling a shell of radius $a = 2$ m. The number of half waves (*m*) of the corresponding mode shape in the direction of the global *Y-axis* is also given in the table.

Table 1. First five dimensionless natural frequencies $\Omega = \omega a^2 \sqrt{\rho\left(1-\nu^2\right)/E}$ for a two span barrel roof and SD boundary conditions on curved boundaries: $h/a = 0.005$, $L/a = 5$, $2\theta = 180^o$.

BC	F-F-F			S-S-S		
mode	DSM	Abaqus	m	DSM	Abaqus	m
1	0.022872	0.022899	(1)	0.076055	0.076147	(1)
2	0.047361	0.047264	(2)	0.078227	0.078319	(1)
3	0.062794	0.062817	(1)	0.081554	0.081646	(1)
4	0.064134	0.064185	(1)	0.111680	0.111865	(1)
5	0.066398	0.066440	(1)	0.116162	0.116393	(1)

Example 2.

Intermediate ring supports are commonly used in cylindrical shell structures to prevent large deformations and excessive vibrations caused by low shell stiffness. To demonstrate the effectiveness of the proposed method, in this example cylindrical shells with ring supports and C-F boundary conditions are studied. Position of the ring supports is shown in Fig. 11. The supports are designed to restrain the tangential and radial displacements *v* and *w*, respectively, i.e. $v = w = 0$.

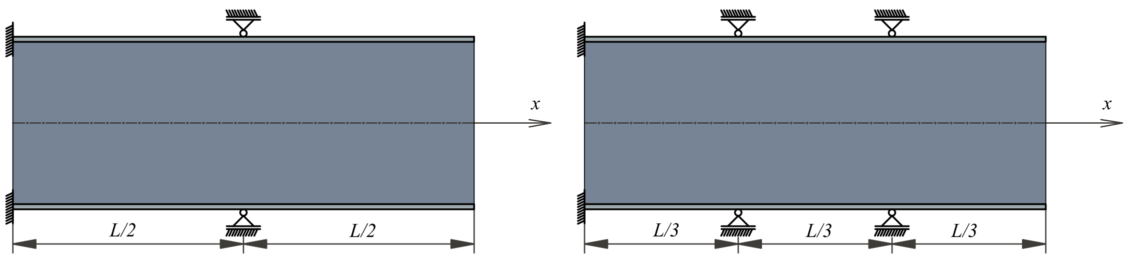

Figure 11. Position of intermediate ring supports for Example 2 (drawing by author, created in AutoCAD)

In Table 2, the first three dimensionless frequency parameters $\Omega = \omega a \sqrt{\rho\left(1-\nu^2\right)/E}$ for $m = 1,2,3,4$ are listed for a shell with one intermediate support and a length-to- radius ratio of 0.5.

The results calculated using the proposed method based on Flügge thin and moderately thick shell theory are compared with those reported by Swaddiwudhipong et al. [13], as well with the results from the FE analysis. Two DS elements are required to model the shell with one intermediate support. Swaddiwudhipong applied the first order approximation theory of Sanders and the FE model consisted of 20120 S4R elements. Excellent agreement is observed between the proposed method based on the moderately thick shell theory and the FEM results, with a maximum relative difference less than 1%. However, the frequencies calculated using presented method based on the Flügge thin shell theory and frequencies reported in [13] are slightly higher, with relative difference reaching up to 13 % for certain modes. This discrepancy is a consequence of neglection of shear deformation. Relatively short shell has significant shear deformation.

Table 3 presents the first three dimensionless frequency parameters for a shell with a length-to-radius ratio of 50, using the proposed method based on Flügge thin and moderately thick shell theory along with the results from Swaddiwudhipong et al. [13] and Jin et al. [14]. Jin employed the FSDT for composite cylindrical shells, while Swaddiwudhipong applied the first order approximation theory of Sanders, as already mentioned. When using DS elements based on the moderately thick shell theory for large length-to-radius ratios, numerical instabilities may occur in MATLAB. The exponential terms in DS matrix become extremely large to be represented with standard floating-point precision. Consequently, for the shell with a length-to-radius ratio of 50, six DS elements were used to ensure numerical stability of the results. An excellent agreement of the results can be observed in the table. The small relative differences, up to 3 % for certain modes, can be attributed to the different shell theories used, as well as to different computational methods applied. Additionally, by comparing the results from Table 2 and Table 3, it can be concluded that as the length-to-radius ratios decrease, the discrepancy between results based on first deformation shell theory and classical shell theory increases.

Table 2. First three dimensionless frequency parameters $\Omega = \omega a\sqrt{\rho\left(1-\nu^2\right)/E}$ *, for C-F circular cylindrical shell with one intermediate ring supports* $(v = w = 0)$*:* $L/a = 0.5$ *,* $h/a = 0.05$ *,* $\nu = 0.3$ *.*

m	Mode	DS Flügge moderately thick	DS Flügge thin	Ref. [13]	Abaqus
1	1	1.0721	1.0903	1.0914	1.0717
	2	3.0862	3.1006	3.1029	3.0878
	3	3.3048	3.6977	3.6988	3.3175
2	1	1.0199	1.0417	1.0435	1.0196
	2	3.0909	3.1013	3.1023	3.0926
	3	3.3291	3.7395	3.7399	3.3418
3	1	0.9699	0.9983	1.1011	0.9697
	2	3.1911	3.1999	3.2005	3.1931
	3	3.3764	3.8094	3.8094	3.3886
4	1	0.9531	0.9913	0.9934	0.9531
	2	3.3795	3.3937	3.3971	3.3838
	3	3.4502	3.9068	3.9066	3.4600

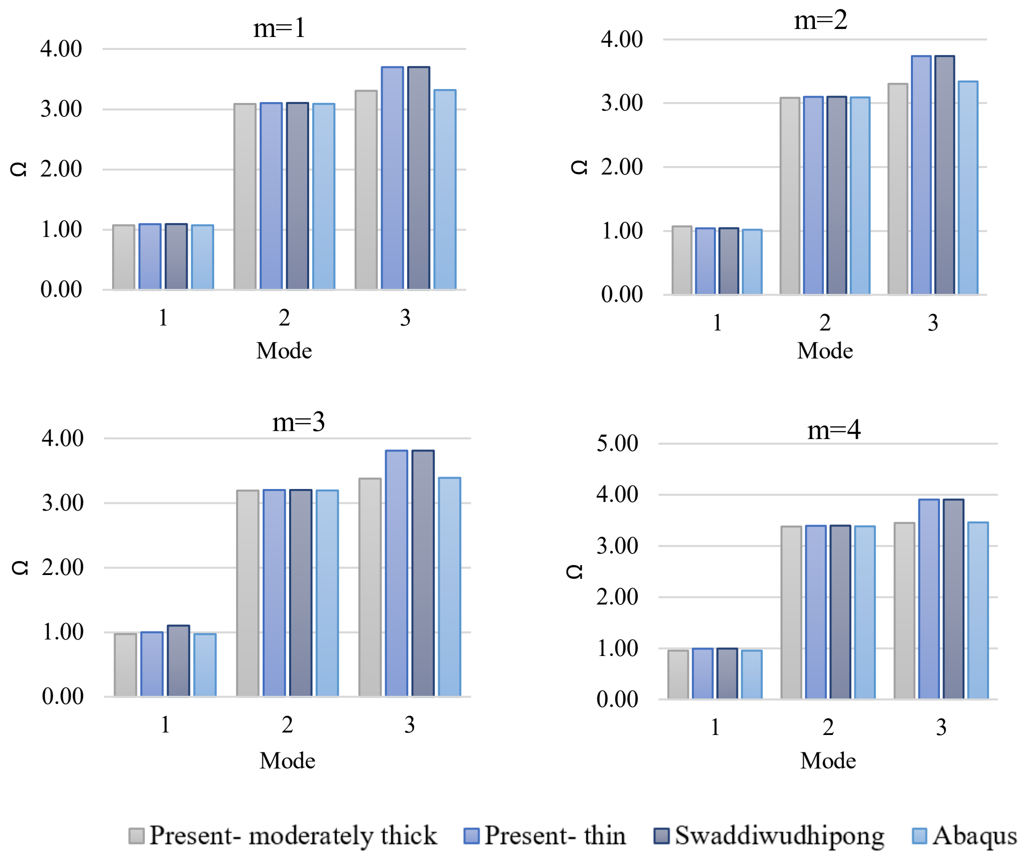

Figure 12. Graphical representation of the results from Table 2

Table 3. First three dimensionless frequency parameters $\Omega = \omega a\sqrt{\rho\left(1-\nu^2\right)/E}$ *, for C-F circular cylindrical shell with one and two intermediate ring supports (*$v = w = 0$ *):* $L/a = 50$, $h/a = 0.05$, $\nu = 0.3$.

m	Mode	one intermediate ring support				two intermediate ring supports			
		DS Flügge moderately thick	DS Flügge thin	Ref. [14]	Ref. [13]	DS Flügge moderately thick	DS Flügge thin	Ref. [14]	Ref. [13]
1	1	0.00263	0.00262	0.00267	0.00267	0.00561	0.00569	0.00569	0.00559
	2	0.01600	0.01596	0.01601	0.01600	0.02869	0.02882	0.02882	0.02911
	3	0.02210	0.02210	0.02245	0.02269	0.03939	0.03986	0.03986	0.03986
2	1	0.03867	0.03873	0.03871	0.03876	0.03876	0.03876	0.03876	0.03883
	2	0.03923	0.03929	0.03928	0.03930	0.04022	0.04028	0.04028	0.04033
	3	0.03964	0.03969	0.03973	0.03975	0.04153	0.04163	0.04163	0.04168
3	1	0.10903	0.10944	0.10912	0.10950	0.10904	0.10918	0.10918	0.10960
	2	0.10938	0.10979	0.10935	0.10980	0.10968	0.10967	0.10967	0.11010
	3	0.10951	0.10992	0.10957	0.10990	0.10986	0.10968	0.10968	0.11030
4	1	0.20828	0.20850	0.20974	0.21000	0.20828	0.20855	0.20855	0.21000
	2	0.20881	0.20873	0.21025	0.21020	0.20908	0.20901	0.20901	0.21050
	3	0.20891	0.20894	0.21035	0.21040	0.20913	0.20911	0.20911	0.21060

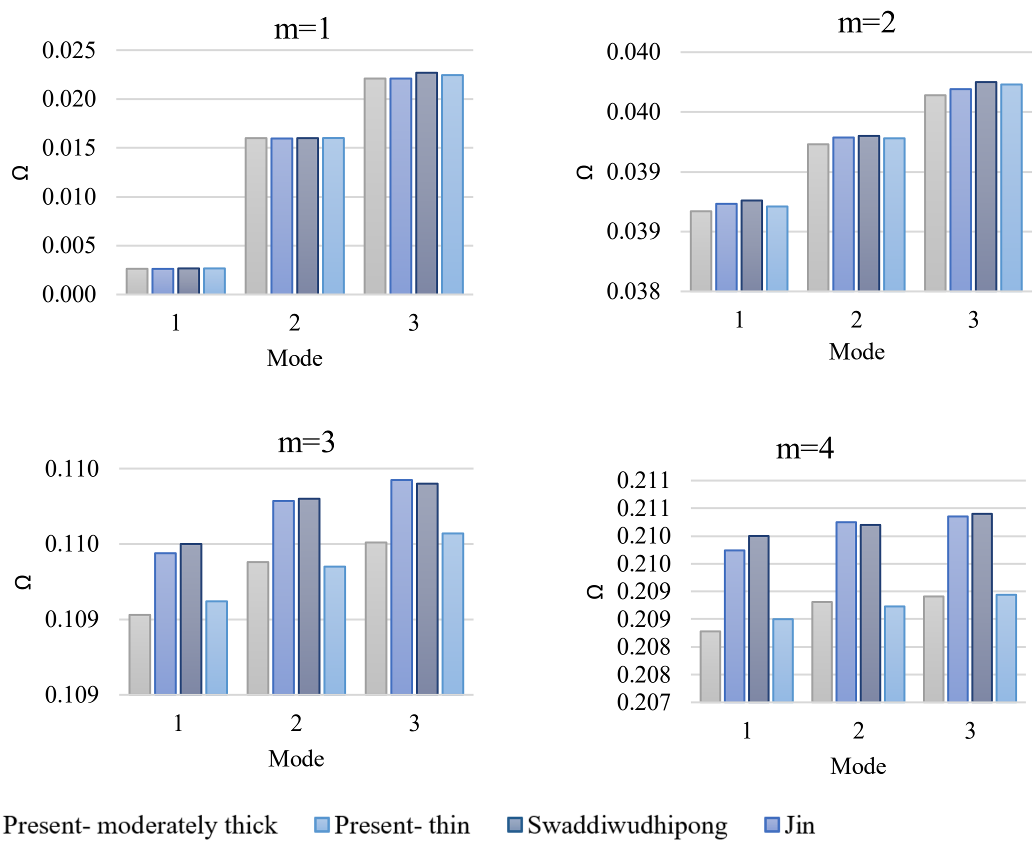

Figure 13. Graphical representation of the results from Table 3 for one intermediate ring support

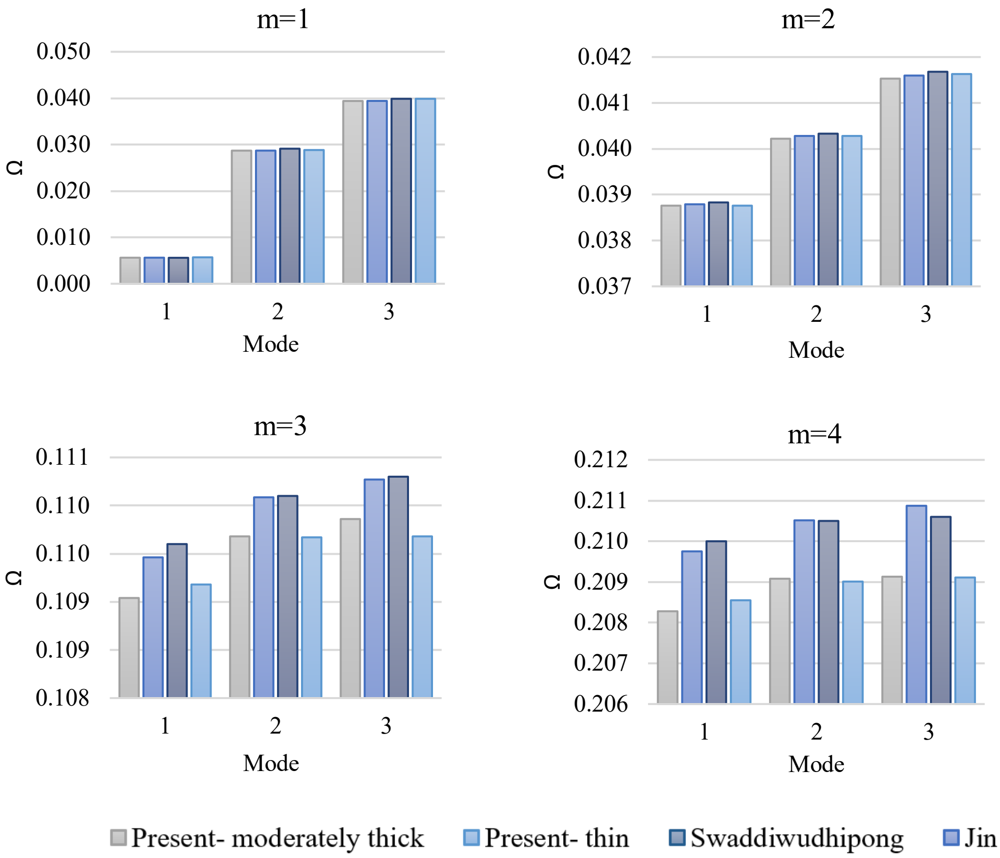

Figure 14. Graphical representation of the results from Table 3 for two intermediate ring support

6. CONCLUSION

This paper presents a review of the authors' contributions to the free vibration analysis of cylindrical shells using the DSM. Formulations of the DS matrix, as the key component of the DSM, for closed circular cylindrical shells based on the classical and moderately thick Flügge shell theories, as well as formulations for shell segments based on the Flügge thin shell theory, are revisited. The assembly procedure of the global DS matrix is outlined and contrasted with the finite element method, emphasizing the coupling of continuous elements at their boundaries. The numerical studies demonstrate the applicability of the DSM to shell-like structures with stepwise thickness variations, intermediate ring supports, barrel roofs, and arbitrary boundary conditions. Comparisons with Abaqus results and data from the literature indicate that the DSM provides high accuracy and computational efficiency in the free vibration analysis of shell-like structures with arbitrary combinations of boundary conditions, regardless of the frequency range. Future work will focus on extending the present formulation to an open circular cylindrical shell based on the moderately thick shell theory, as well as on accounting for more general boundary conditions modeled by elastic restraints. In addition, the influence of the foundation stiffness and soil–structure interaction effects will be investigated within the DSM framework.

LITERATURE

[1] R. S. Langley, "A dynamic stiffness technique for the vibration analysis of stiffened shell structures," *Journal of Sound and Vibration,* vol. 156, no. 3, p. 521–40, 1992.

[2] A. Y. Leung, W. E. Zou, "Dynamic Stiffness Analysis of Circular Cylindrical Shells," *International Society of Offshore and Polar Engineers,* 1993.

[3] A. Leung, N. Kwok, "Dynamic stiffness analysis of toroidal shells," *Thin-Walled Structures,* vol. 21, no. 1, pp. 43-64, 1995.

[4] J. B. Casimir, M. C. Nguyen, I. Tawfiq, "Thick shells of revolution: Derivation of the dynamic stiffness matrix of continuous elements and application to a tested cylinder," *Computers & Structures,* vol. 85, pp. 1845-1857, 2007.

[5] T. I. Thinh, M. C. Nguyen, "Dynamic stiffness matrix of continuous element for vibration of thick cross-ply laminated composite cylindrical shells," *Composite Structures,* vol. 98, pp. 93-102, 213.

[6] D. Tounsi, J. B. Casimir, S. Abid, I. Tawfiq, M. Haddar, "Dynamic stiffness formulation and response analysis of stiffened shells," *Computers & Structures,* vol. 132, pp. 75-83, 2014.

[7] F. A. Fazzolari, "A refined dynamic stiffness element for free vibration analysis of cross-ply laminated composite cylindrical and spherical shallow shells," *Composites Part B: Engineering,* vol. 62, pp. 143-158, 2014.

[8] N. Kolarević, M. Nefovska-Danilović, M. Petronijević. , "Metoda dinamičke krutosti u analizi vibracija kružne cilindrične ljuske," *Građevinski materijali i konstrukcije ,* vol. 59(3), pp. 45-62, 2016.

[9] Nevenka Kolarević, Marija Nefovska-Danilović, "Dynamic stiffness–based free vibration study of moderately thick circular cylindrical shells," *Thin-Walled Structures,* vol. 218, no. Part B, 2026.

[10] Kolarević N, Nefovska-Danilović M., "Dynamic stiffness – based free vibration study of open circular cylindrical shells," *Journal of Sound and Vibration,* vol. 486, 2020.

[11] A. W. Leissa, Vibration of shells, Washington, D.C: US Government Printing Office, 1973.

[12] S. Kevorkian, M. Pascal, "An accurate method for free vibration analysis of structures with application to plates," *Journal of Sound and Vibration,* vol. 246, no. 5, pp. 795-814, 2001.

[13] S. Swaddiwudhipong,J.Tian, C.M. Wang, "Vibration of cylindrical shells with intermediate ring supports," *Journal of Sound and Vibration,* vol. 187, no. 1, p. 69–93, 1995.

[14] G Jin, T. Ye, X.L.Ma, Y.H. Chen, Z. Su, X. Xi, "A unified approach for the vibration analysis of moderately thick composite laminated cylindrical shells with arbitrary boundary conditions," *International Journal of Mechanical Sciences ,* vol. 75, p. 357–376, 2013.